Electronic Coupling in a Synthetic Model of the Cu–Cofactor Unit

of the P_M State in Cytochrome *c* Oxidase

Sang Tae Lee[a], Christopher G. Bailey[b, c], Daniel A. Santos[a], Mohan Bhadbhade[d], Heejin Kim[e*], and Dong Jun Kim[a*]

[a]*School of Chemistry, University of New South Wales, Sydney, NSW 2052, Australia*

[b]*School of Physics, The University of Sydney, Sydney, NSW 2006, Australia*

[c]*Sydney Nano, The University of Sydney, Sydney, NSW 2006, Australia*

[d]*Mark Wainwright Analytical Centre, University of New South Wales, Sydney, NSW 2052, Australia*

[e]*Research Center for Materials Analysis, Korea Basic Science Institute, Daejeon 34133, Republic of Korea*

* Email: heejinkim@kbsi.re.kr; dongjun.kim@unsw.edu.au

Supplementary Information

Section A. Synthetic Protocols

1) Synthesis of Im-Hq, [Cu^{II}(terpy)(Im-Hq)]$^{2+}$ and [Cu^{II}(terpy)(Im-Q)]$^{2+}$

All starting materials and reagents were purchased from commercial suppliers (Aldrich and Chem-Supply Pty Ltd.) and used without further purification. Cofactors using a phenol moiety employ either the nucleophilic substitution of a halogenated aryl precursor with imidazole,[1,2] or a method using a lead acetate substitution.[3] A quinone moiety allows the use of an imidazole-coupling method described by Escolastico et. al.[4] *2-Acetyl-1,4-benzoquinone* (**2**) was synthesised using modified methods previously described in literature.[5] ^{1}H NMR (400 MHz, CDCl$_3$) δ 7.00 (1H, d, Ar), 6.81 (1H, d, Ar), 6.80 (1H, s, Ar), 2.55 (3H, s, CH$_3$).

1) *1-(2'-Acetyl-3',6'-hydroquinone)imidazole* (**3**)

Quinone **2** (407 mg, 2.71 mmol) in chloroform (1.2 mL) was added slowly to imidazole (185 mg, 1 eq.) in chloroform (1.2 mL). The reaction mixture was stirred for 3 hours at room temperature. The colour changed from red to green-yellowish. The solvent was removed on a rotary evaporator. The solid was dissolved in ethanol and diethyl ether was added. A white precipitate was formed, which was filtered over celite and the filtrate collected. The solvent was removed using a rotary evaporator. Diethyl ether was added to give a yellowish-green precipitate. (0.48 g, 94 %). ^{1}H NMR (400 MHz, DMSO-d_6) δ 9.72 (1H, s, OH), 9.53 (1H, s, OH), 7.56 (1H, s, Im), 7.11 (1H, s, Im), 6.97 (1H, d, Ar), 6.93 (1H, s, Im), 6.86 (1H, d, Ar), 2.21 (3H, s, CH3); ^{13}C NMR (100 MHz, DMSO-d_6) 201.55, 147.08, 145.65, 138.95, 128.29, 127.92, 122.24, 121.48, 118.56, 117.60, 31.95, shown in Supplementary Figure 1; ν cm^{-1} 3426br, 3132m, 1638s, 1580s, 1505s, 1466s, 1422w, 1298s, 1224s, 1196s, 1066s, shown in Supplementary Figure 2.

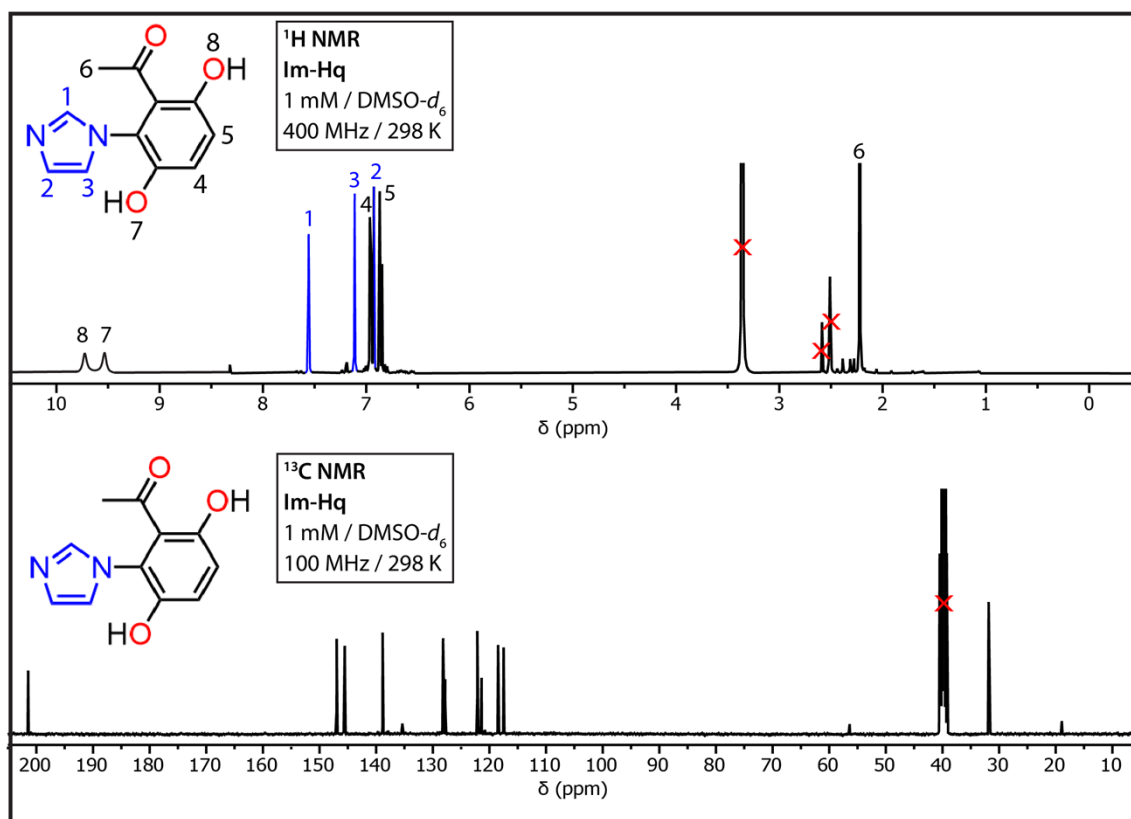### 2) *[Cu^{II}(terpy)(Im-Hq)](ClO$_4$)$_2$* (**4**)

Cu(ClO$_4$)$_2$•6H$_2$O (37.05 mg, 1 eq.) in methanol (1.0 mL) was added to terpy (23.3 mg, 1 eq.) in methanol (1 mL) followed by the addition of **3** (21.8 mg, 0.1 mmol) in methanol (1.2 mL). The mixture was stirred for 10 min at room temperature and then filtered. The filtrate was placed under a diethyl ether atmosphere for several days to give blue crystalline plates (64 mg, 90 %). ESI-MS (MeCN, positive ion mode): m/z 257.0476 (C$_{26}$H$_{21}$CuN$_5$O$_3{}^{2+}$, 100.0%); calcd. for C$_{26}$H$_{21}$CuN$_5$O$_3{}^{2+}$ 257.04647. $\lambda_{max/nm}$ (MeCN) 638 (ε = 133 L mol^{-1} cm^{-1}), 339 (7,738, sh), 326 (8,086), 285 (8,022), shown in Supplementary Figure 2. FT-IR: ν/cm^{-1} 3350br, 3123w, 1635s, 1477s, 1451s, 1253m, 1052s. EPR (frozen MeOH solution, 77 K): g∥ = 2.249, g⊥ = 2.050, A∥ (Cu) = 153 G.

3) *[Cu^{II}(terpy)(Im-Q)](ClO$_4$)$_2$* (**5**)

A mixture of **4** (29.88 mg, 0.042 mmol) and Ag$_2$O (29 mg, 3 eq.) in acetonitrile (4.0 mL) was stirred for 2 hours at room temperature. The filtrated green solution on celite was placed under a diethyl ether atmosphere for several days to give green crystalline plates. The obtained crystals decomposed readily upon recrystallisation and, because only a small amount of material was available, were used solely for single-crystal X-ray diffraction analysis.

Section B. NMR and EPR Spectroscopy

1) NMR Characterisation of Im-Hq

Supplementary Figure 1: ^{1}H and ^{13}C NMR Spectra of **Im-Hq** (400 and 100 MHz, DMSO-d_6)

2) Laser-induced EPR Spectroscopy

EPR spectra were recorded on frozen samples in fused-quartz tubes at 100 K using a Bruker ELEXSYS-II E580 spectrometer with a microwave frequency of 9.615 GHz and a power of 0.15 mW. Temperature control was provided by a closed-cycle helium EPR cryostat (Cryogenics Ltd.). Lock-in detection was used to acquire the first-derivative signal with a magnetic-field modulation amplitude of 0.1 mT (1 G) at 100 kHz. Illumination was provided using the 355 nm output from a pulsed laser source (Opotek Opolette) operating at 20 Hz. The pulse energy was ~18 mJ with a pulse width of ~4 ns.

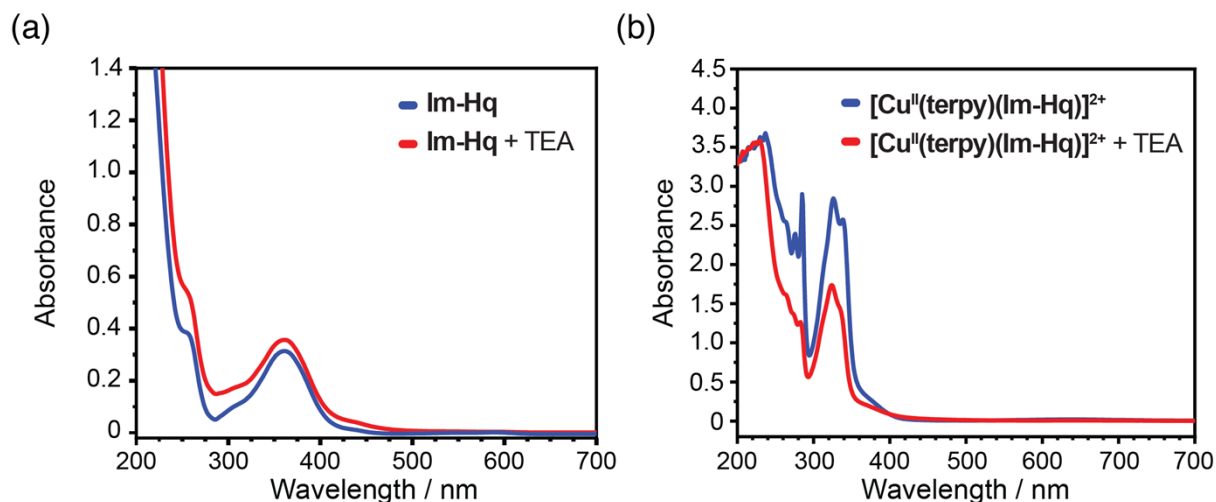## Section C. Single Crystal X-ray Crystallography

1) Crystal structures of **Im-Hq**, **[Cu^{II}(terpy)(Im-Hq)](ClO$_4$)$_2$** and **[Cu^{II}(terpy)(Im-Q)](ClO$_4$)$_2$**

X-ray quality crystals were grown by slow vapor diffusion of diethyl ether into a solution in MeCN/MeOH, while crystals of **Im-Hq** were grown by slow evaporation from methanol. Suitable single crystals were selected under the polarizing microscope (Leica M165Z), mounted on a MicroMount (MiTeGen, USA) consisting of a thin polymer tip with a wicking aperture. The X-ray diffraction measurements were carried out on a Bruker D8 Quest Single Crystal diffractometer with Photon II detector at 100 K by using IμS 3.0 Microfocus Source with Mo-Kα radiation ($\lambda = 0.710723$ Å) . The single crystal, mounted on the goniometer using cryo loops for intensity measurements, was coated with paraffin oil and then quickly transferred to the cold stream using an Oxford Cryo stream 800 attachment. Symmetry related absorption corrections using the program SADABS[6] were applied and the data were corrected for Lorentz and polarisation effects using Bruker APEX3 software.[6] The structure was solved by ShelxT (intrinsic phasing)[7] and the full-matrix least-square refinement was carried out using Shelxl[8] in Olex2[9]. The non-hydrogen atoms were refined anisotropically. The molecular graphic was generated using program Olex2.[9]

	Im-Hq	**[Cu^{II}(terpy)(Im-Hq)](ClO$_4$)$_2$**	**[Cu^{II}(terpy)(Im-Q)](ClO$_4$)$_2$**
CCDC Number	2432274	2432390	2432275
Chemical formula	C$_{11}$H$_{10}$N$_2$O$_3$	C$_{26}$H$_{21}$Cl$_{0.5}$CuN$_5$O$_5$·1.5(ClO$_4$)	C$_{26}$H$_{19}$CuN$_5$O$_3$·2(ClO$_4$)·C$_2$H$_3$N
M_r	218.21	713.92	752.95
Crystal system, space group	Monoclinic, $P2_1/n$	Monoclinic, $C2/c$	Triclinic, $P\overline{1}$
Temperature (K)	150	122	120
a, b, c (Å)	7.8990 (5), 10.5835 (11), 12.1200 (9)	16.2136 (7), 8.2399 (3), 41.7295 (13)	8.4620 (11), 12.2061 (17), 16.491 (3)
ß (°)	102.187 (7)	98.216 (3)	77.652 (9)
α, γ (°)			69.700 (9), 72.490 (9)
V (Å^3)	990.39 (14)	5517.8 (4)	1512.1 (4)
Z	4	8	2
Radiation type	Cu $K\alpha$	Cu $K\alpha$	Cu $K\alpha$
μ (mm^{-1})	0.91	3.55	3.29
Crystal size (mm)	0.08 × 0.04 × 0.01	0.05 × 0.05 × 0.02	0.02 × 0.04 × 0.08
Diffractometer	ROD, Synergy Custom DW system, HyPix	Bruker D8 Quest	Bruker D8 Quest
Absorption correction	Gaussian *CrysAlis PRO* 1.171.43.127a (Rigaku Oxford Diffraction, 2024) Numerical absorption correction based on gaussian integration over a multifaceted crystal model Empirical absorption correction using spherical harmonics, implemented in SCALE3 ABSPACK scaling algorithm.	Multi-scan *SADABS2016*/2 (Bruker,2016/2) was used for absorption correction. wR2(int) was 0.1073 before and 0.0815 after correction. The Ratio of minimum to maximum transmission is 0.7544. The λ/2 correction factor is Not present.	Multi-scan *SADABS2016*/2 (Bruker,2016/2) was used for absorption correction. wR2(int) was 0.1592 before and 0.1009 after correction. The Ratio of minimum to maximum transmission is 0.6682. The ë/2 correction factor is Not present.
T_{min}, T_{max}	0.942, 1.000	0.567, 0.752	0.502, 0.752
No. of measured, independent and observed [$I > 2\sigma(I)$] reflections	5693, 1886, 1169	53923, 4259, 3826	29155, 4298, 2320
R_{int}	0.048	0.079	0.243
θ_{max} (°)		61.3	59.9
$(\sin \theta/\lambda)_{max}$ (Å^{-1})	0.618	0.569	0.561
$R[F^2 > 2\sigma(F^2)]$, $wR(F^2)$, S	0.050, 0.131, 1.03	0.061, 0.135, 1.17	0.071, 0.202, 1.03
No. of reflections	1886	4259	4298
No. of parameters	148	700	435
No. of restraints		694	
H-atom treatment	H-atom parameters constrained	H-atom parameters constrained	H-atom parameters constrained
		$w = 1/[\sigma^2(F_o^2) + (0.0271P)^2 + 38.8822P]$ where $P = (F_o^2 + 2F_c^2)/3$	
$\Delta\rho_{max}$, $\Delta\rho_{min}$ (e Å^{-3})	0.16, -0.20	0.58, -0.47	0.53, -0.57

Computer programs: *SAINT* V8.40B (2016), *SHELXT* 2018/2 (Sheldrick, 2018), *SHELXL* 2018/3 (Sheldrick, 2015),

Olex2 1.5 (Dolomanov *et al.*, 2009).

Section D. UV-Visible Spectrophotometry

(a)

(b)

Supplementary Figure 2: UV-vis spectra of **Im-Hq** and **[Cu^{II}(terpy)(Im-Hq)]$^{2+}$.** (a) UV-vis spectra of **Im-Hq** (1 mM, blue) and **Im-Hq** with 3 equivalents of triethylamine (TEA, red) in MeCN. (b) UV-vis spectra of **[Cu^{II}(terpy)(Im-Hq)]$^{2+}$** (1 mM, blue) and **[Cu^{II}(terpy)(Im-Hq)]$^{2+}$** with 3 equivalents of TEA (red) in MeCN.
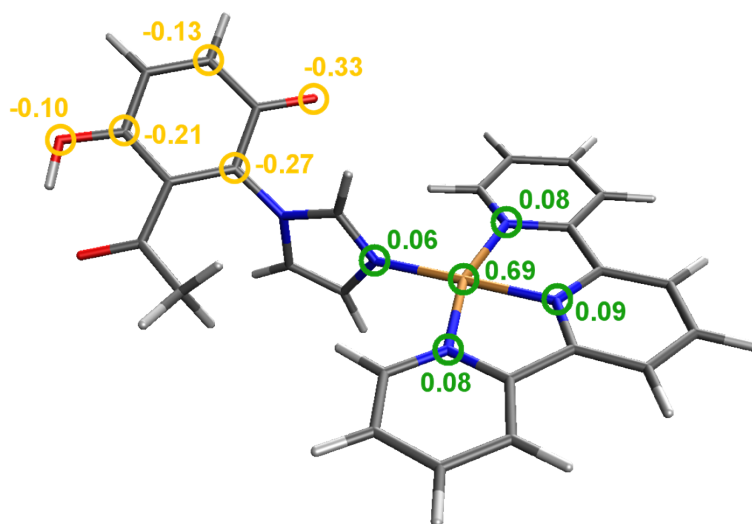
UV–vis spectra were recorded for 1 mM solutions of **Im-Hq**, **Im-Hq** with 3 equivalents of TEA, and **[Cu^{II}(terpy)(Im-Hq)]$^{2+}$** using a Jasco V-730 spectrophotometer and a quartz cuvette. **Im-Hq** shows a characteristic absorption band at 360 nm. Upon addition of base (3 equivalents of TEA), the absorption at 360 nm increases. **[Cu^{II}(terpy)(Im-Hq)]$^{2+}$** displays absorption bands at 330 and 280 nm, corresponding to the hydroquinone moiety and the terpyridine ligand, respectively.

FT-IR spectra of **Im-Hq** and **[Cu^{II}(terpy)(Im-Hq)]$^{2+}$** were recorded on a PerkinElmer Spectrum Two FT-IR spectrometer.
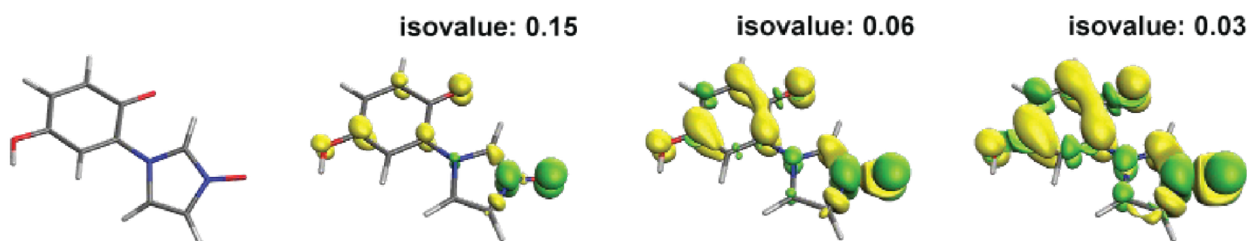
Section E. Computational Studies

Computational details. DFT calculations were performed using the B3LYP functional[10] as implemented in Q-Chem software.[11] The basis sets employed were 6-31g* for Cu, 6-311+g* for O, 6-31+g* for N and H, and 6-31g* for C atoms.[12] A polarisable continuum model[13] was applied to represent the acetonitrile solvent implicitly (dielectric constant: 37.5). The spin density isosurfaces were visualized using IQmol software. To obtain the broken-symmetry state, we first performed

geometry optimisation with the CDFT approach. Standard DFT calculations were then carried out using this optimised geometry as the starting point, which yielded the same spin state but at a lower energy.

Supplementary Figure 3: Spin population values for atoms with high spin density. Green and yellow numbers are excess up and down spin, respectively.

Supplementary Figure 4: [O-Im-Sq] model system and its spin density maps at isovalues of 0.15, 0.06, and 0.03. Blue, red, grey, and white bars represent N, O, C, and H atoms, respectively. Green and yellow surfaces indicate excess up and down spin density, respectively.

Section F. References

1   Kiyomori, A., Marcoux, J.-F. & Buchwald, S. L. An efficient copper-catalyzed coupling of aryl halides with imidazoles. *Tetrahedron Lett* **40**, 2657-2660 (1999).

2   Klapars, A., Antilla, J. C., Huang, X. & Buchwald, S. L. A General and Efficient Copper Catalyst for the Amidation of Aryl Halides and the N-Arylation of Nitrogen Heterocycles. *J Am Chem Soc* **123**, 7727-7729 (2001).

3   Elliott, G. I. & Konopelski, J. P. Complete N-1 Regiocontrol in the Formation of N-Arylimidazoles. Synthesis of the Active Site His-Tyr Side Chain Coupled Dipeptide of Cytochrome c Oxidase. *Org Lett* **2**, 3055-3057 (2000).

4   Escolástico, C. *et al.* Imidazole and benzimidazole addition to quinones. Formation of meso and d,l isomers and crystal structure of the d,l isomer of 2,3-Bis(benzimidazol-1'-yl)-1,4-dihydroxybenzene. *Tetrahedron* **50**, 12489-12510 (1994).

5   Kuser, P., Frauenfelder, E. F. & Eugster, C. H. Anlagerung von Enoläthern, Acetylenäthern und Heterocyclen an 2-Acetyl-1,4-benzochinon. *Helv Chim Acta* **54**, 969-979 (1971).

6   Bruker (2016). APEX3, S. a. S. B. A. I., Madison, Wisconsin, USA.

7   Sheldrick, G. SHELXT - Integrated space-group and crystal-structure determination. *Acta Crystallogr A* **71**, 3-8 (2015).

8   Sheldrick, G. Crystal structure refinement with SHELXL. *Acta Crystallogr C* **71**, 3-8 (2015).

9   Dolomanov, O. V., Bourhis, L. J., Gildea, R. J., Howard, J. A. K. & Puschmann, H. OLEX2: a complete structure solution, refinement and analysis program. *J Appl Crystallogr* **42**, 339-341 (2009).

10   Becke, A. D. A new mixing of Hartree–Fock and local density-functional theories. *J Chem Phys* **98**, 1372-1377 (1993).

11   Shao, Y. *et al.* Advances in molecular quantum chemistry contained in the Q-Chem 4 program package. *Mol Phys* **113**, 184-215 (2015).

12   Schaefer, A. W., Roveda, A. C., Jr., Jose, A. & Solomon, E. I. Geometric and electronic structure contributions to O-O cleavage and the resultant intermediate generated in heme-copper oxidases. *J Am Chem Soc* **141**, 10068-10081 (2019).

13   Barone, V. & Cossi, M. Quantum calculation of molecular energies and energy gradients in solution by a conductor solvent model. *J Phys Chem A* **102**, 1995-2001 (1998).